A core top assessment of proxies for the ocean carbonate system in surface-dwelling foraminifers

Yunyan Ni,[1,2] Gavin L. Foster,[1] Trevor Bailey,[3] Tim Elliott,[1] Daniela N. Schmidt,[4] Paul Pearson,[5] Brian Haley,[1,6] and Chris Coath[1]

Received 28 June 2006; revised 14 March 2007; accepted 21 May 2007; published 18 August 2007.

[1] We have assessed the reliability of several foraminifer-hosted proxies of the ocean carbonate system (δ^{11}B, B/Ca, and U/Ca) using Holocene samples from the Atlantic and Pacific oceans. We examined chemical variability over a range of test sizes for two surface-dwelling foraminifers (*Globigerinoides sacculifer* and *Globigerinoides ruber*). Measurements of δ^{11}B in *G. ruber* show no significant relationship with test size in either Atlantic or Pacific sites and appear to provide a robust proxy of surface seawater pH. Likewise there is no significant variability in the δ^{11}B of our Atlantic core top *G. sacculifer*, but we find that δ^{11}B increases with increasing test size for *G. sacculifer* in the Pacific. These systematic differences in δ^{11}B are inferred to be a consequence of isotopically light gametogenic calcite in *G. sacculifer* and its preferential preservation during postdepositional dissolution. The trace element ratio proxies of ocean carbonate equilibria, U/Ca and B/Ca, show systematic increases in both *G. ruber* and *G. sacculifer* with increasing test size, possibly as a result of changing growth rates. This behavior complicates their use in paleoceanographic reconstructions. In keeping with several previous studies we find that Mg/Ca ratios increase with increasing size fraction in our well-preserved Atlantic *G. sacculifer* but not in *G. ruber.* In contrast to previous interpretations we suggest that these observations reflect a proportionally larger influence of compositionally distinct gametogenic calcite in small individuals compared to larger ones. As with δ^{11}B this influences *G. sacculifer* but not *G. ruber*, which has negligible gametogenic calcite.

Citation: Ni, Y., G. L. Foster, T. Bailey, T. Elliott, D. N. Schmidt, P. Pearson, B. Haley, and C. Coath (2007), A core top assessment of proxies for the ocean carbonate system in surface-dwelling foraminifers, *Paleoceanography*, *22*, PA3212, doi:10.1029/2006PA001337.

1. Introduction

[2] The sensitivity of the Earth's climate to pCO_2 is a hotly debated topic, and proxy data for past pCO_2 has a direct bearing on this problem. Boron isotopic measurements in marine foraminiferal calcite have been used as a proxy of oceanic pH and hence a means of assessing past changes in pCO_2 [e.g., *Hönisch and Hemming*, 2005]. Yet previous work has highlighted observational and theoretical evidence for variability of boron isotope ratios (δ^{11}B) related to foraminiferal test size [e.g., *Hönisch and Hemming*, 2004], which hinders the application of the B isotope proxy in paleoceanography. Furthermore, pH alone is not sufficient to fully constrain the state of the oceanic carbonate equilibrium and so ideally an additional proxy, for example of [CO_3^{2-}], needs to be measured in tandem with δ^{11}B.

[3] We address these issues by performing a core top (Holocene) study of δ^{11}B and other trace element proxies of the carbonate system, notably U/Ca and B/Ca. In combination with additional trace element abundances (Li, Mg and Sr) we provide constraints on the process of calcification and how it influences the proxies of the carbonate system. We have analyzed a range of different test sizes of *G. sacculifer* and *G. ruber* (white and pink) from the western equatorial Pacific (ODP Site 806B) and central equatorial Atlantic (ODP Site 664C). We further measured δ^{11}B of *G. sacculifer* in the Indian (RC 14-37PC) Ocean. We have focused on two surface-dwelling species of tropical/subtropical foraminifers, as these are likely the most important in reconstructing records of pCO_2. The three sites have different temperatures and carbonate saturation and hence allow the influence of different environmental conditions to be tested.

2. Material and Methods

[4] Holocene foraminifers were picked from two sites: ODP Site 806B from the Ontong Java Plateau in the equatorial Pacific and ODP site 664C in the central equatorial Atlantic. Additionally we analyzed *G. sacculifer* picked and supplied by B. Hönisch from RC 14-37PC on the 90-East Ridge, Indian Ocean. This was primarily done as an interlaboratory comparison but also provides data from a third ocean basin. The sedimentation rate is 2.2 cm/kyr

[1]Bristol Isotope Group, Department of Earth Sciences, University of Bristol, Bristol, UK.
[2]Now at Research Institute of Petroleum Exploration and Development, Beijing, China.
[3]National Museums and Galleries of Wales, Cardiff, UK.
[4]Department of Earth Sciences, University of Bristol, Bristol, UK.
[5]School of Earth, Ocean and Planetary Sciences, Cardiff University, Cardiff, UK.
[6]Now at IFM-GEOMAR, Kiel, Germany.

0883-8305/07/2006PA001337

Table 1. Sediment Core Locations, Sampling Depths, and Foraminiferal Biometric Data

Core	Latitude	Longitude	Water Depth, m	Depth in Core, cm	Species	Symbiont	Size Fractions, μm
806B	0°19.1′N	159°21.7′E	2520	12	*G. sacculifer*[a]	dinoflagellate	600–700, 500–600, 425–500, 355–425, 300–355, and 250–300
806B	0°19.1′N	159°21.7'E	2520	12	*G. ruber*[b]	dinoflagellate	355–425, 300–355, 250–300, and 200–250
664C	0°07′N	23°14′W	3806	10	*G. sacculifer*[a]	dinoflagellate	600–700, 500–600, 425–500, 355–425, 300–355, 250–300, and 212–250
664C	0°07′N	23°14′W	3806	10	*G. ruber*[b]	dinoflagellate	425–500, 355–425, 300–355, 250–300, 212–250, and 180–212
664C	0°07′N	23°14′W	3806	10	*G. ruber*[c]	dinoflagellate	425–500, 355–425, 300–355, 250–300, 212–250, and 180–212
RC14-37	1.5°N	90.2°E	2230	4	*G. sacculifer*[a]	dinoflagellate	515–865, 425–515, 380–425, and 250–350

[a] *G. sacculifer* with final sac-like chamber.
[b] *G. ruber* white.
[c] *G. ruber* pink.

for ODP site 806B [*Berger et al.*, 1993], 3.7 cm/kyr over the last 1.3 Myr for ODP site 664C [*Raymo et al.*, 1997] and 1–2 cm/kyr for RC 14-37PC [*Peterson and Prell*, 1985]. The Holocene age of these samples has been confirmed by the oxygen isotope stratigraphy of all three sites [*Berger et al.*, 1993; *Peterson and Prell*, 1985; *Raymo et al.*, 1997]. Further site details are reported in Table 1.

[5] Sediment samples were washed, sieved and dried. Depending on the size fraction and abundance, 25–120 individuals (typically ~1.3 mg of calcium carbonate) of *G. sacculifer* (with final sac-like chamber) and *G. ruber* (white and pink) were picked from the 180 to 710 μm size fractions (Table 1). Not all species could be found in each size fraction. The size fractions cited relate to the sieve size, not direct size measurements. Specimens from all samples and size fractions were examined with a scanning electron microscope, confirming that all specimens of *G. sacculifer* have undergone gametogenesis and produced a thick gametogenic calcite crust indicative of the final stage of the foraminiferal life cycle.

[6] The foraminifer cleaning protocol followed here was designed principally with boron isotopes in mind and is described in detail by *Foster et al.* [2006]. We are most concerned with cleaning steps that ensure a good separation between the carbonate and unwanted clays which may influence the measured δ^{11}B [*Deyhle and Kopf*, 2004]. To this end, after crushing the foraminifers between precleaned glass plates, we followed the clay removal approach outlined by *Barker et al.* [2003]. Neither boron nor the other trace elements of interest here are present in high concentrations in Fe-Mn oxides that frequently coat ocean sediments (e.g., B/Mn < 4 mmol/mol [*Axelsson et al.*, 2002]). Even when high Mn/Ca ratios are measured in sedimentary foraminifera (e.g., 500 μmol/mol) boron concentrations and isotope ratios are unlikely to be significantly influenced given the high typical boron concentration in foraminifera (>80 μmol/mol). We therefore chose not to use a reductive step [e.g., *Boyle and Keigwin*, 1985] to remove the Fe-Mn coatings, particularly since the samples investigated here are all core top and have Mn/Ca ratios <50 μmol/mol (see below). Following other boron isotope studies [e.g., *Hönisch and Hemming*, 2005] organic material was oxidized by bleaching the samples in sodium hypochlorite (NaClO; 5% Cl) for 24 hours following clay removal. For those trace element ratios investigated here it was found that this approach yielded similar results to the buffered H_2O_2 approach of *Barker et al.* [2003].

[7] The boron isotopic compositions of foraminiferal separates were determined using total evaporation negative-ion thermal ion mass spectrometry (TE-NTIMS). This methodology allows smaller sample sizes to be measured and in a more routine manner than traditional N-TIMS. Our TE-NTIMS measurements are within the wide range of previous N-TIMS measurements of equivalent core top foraminifera, but notably some 3‰ heavier relative to the most recent measurements of *Hönisch and Hemming* [2004, 2005]. Nevertheless, other studies have emphasized that isotopic differences between samples rather than their delta value (relative to the pure NBS 951 boric acid standard) are most significant and our difference between *G. sacculifer* and *Orbulina universa* of ~3‰ is in good agreement with other conventional N-TIMS studies [*Sanyal et al.*, 1996, 2000; *Hönisch et al.*, 2003]. The analytical details of our TE-NTIMS approach are as described by *Foster et al.* [2006]. During the course of this study the long-term reproducibility of the boron isotopic composition of our in-house foraminiferal carbonate standard (871std) was 18.1 ± 1.2‰ (2 standard deviations of the mean (SD); n = 95). The reproducibility for separately prepared samples is in some cases better than ±1‰ (2 SD) and for repeat of the same sample solutions it is typically better than ±1‰ (2 SD).

[8] Tandem elemental analysis (see below) with boron isotopic measurements allowed screening of samples in which clay had not been sufficiently removed during cleaning. We used a criteria of Al/Ca < 100 μmol/mol as an indication of properly cleaned samples. Of the few samples that failed this test, some had δ^{11}B several permil lower than correctly cleaned samples.

[9] This study differs from other boron isotope investigations in that trace element ratios and boron isotopes were measured on the same separated fraction of foraminifers. An aliquot of the solution prepared for boron isotope analysis was analyzed on a ThermoFinnigan Element 2 Inductively Coupled Plasma Mass Spectrometer (ICP-MS) at the University of Bristol. The analytical protocol followed

Table 2. A Comparison Between B/Ca Ratio by Isotope Dilution and Element 2

	B/Ca,[a] μmol/mol	2 SD, %	[B],[b] μmol/L	$[Ca]_{weight}$,[c] mmol/L	B/Ca_{weight},[d] μmol/mol	$[Ca]_{element}$,[e] mmol/L	$B/Ca_{element}$,[f] μmol/mol	$\Delta_{B/Ca}$,[g] %
BSGS+boron	85.89	2.10	2068.13	24.24			85.33	0.65
871 all	74.83	3.16	0.05	0.70	75.90	0.71	75.29	−0.62
871 300–355	70.04	3.50	0.02	0.26	74.68	0.26	73.84	−5.43
999 425–500	67.97	2.94	0.03	0.47	67.09	0.46	69.04	−1.58
999 500–600	65.03	3.26	0.02	0.28	67.60	0.29	66.95	−2.95

[a]B/Ca values measured on the Element 2 ICPMS.
[b]Boron concentration determined using isotope dilution using NIST SRM 952 boric acid.
[c]$[Ca]_{weight}$ calcium concentration determined using weight of dissolved foraminifers and acid used for dissolution.
[d]B/Ca_{weight} calcium values determined by weighing.
[e]$[Ca]_{element}$ calcium concentration determined on the Element 2.
[f]$B/Ca_{element}$ calcium values determined on Element 2.
[g]$\Delta_{B/Ca}$ deviation of the two methods, ICPMS and isotope dilution.

Rosenthal et al. [1999] including a matrix correction. We ran samples against our own gravimetrically prepared solutions from concentrated stocks (purchased from CPI International). For Ca, Sr, Mg, U, our in-house (BSGS) standard was intercalibrated against a split of the Rutgers standard supplied by Y. Rosenthal, for which we obtained good agreement (within 2% for Mg/Ca). The precision of measured Mg/Ca ratios was <0.09 mmol/mol (2 SD) for a standard solution of Mg/Ca = 5.381 mmol/mol. The long-term reproducibility for Mg/Ca is estimated as ±1.4% (2 SD) based on 42 runs of the three "consistency standards" over a one and a half year period. The consistency standards are made up from the same elemental stock solutions and have the same Ca concentration as the primary reference standard but are made with different trace element/Ca ratios. The average reproducibility of Mg/Ca ratios of repeat dissolutions of samples is ±2% (2 SD), ±1.5% (2 SD) for Sr/Ca, and ±5% (2 SD) for both Li/Ca and U/Ca.

[10] For B/Ca we use a slightly modified approach because of the well-documented memory problem associated with measuring boron by ICPMS [see *Al-Ammar et al.*, 2000]. The problem stems from volatization of boric acid from the sample solution which coats the walls of the spray chamber in the ICPMS introduction system and results in unacceptable washout times between samples (e.g., >20 min to wash to 1% background). To overcome this memory problem we follow the approach of *Al-Ammar et al.* [2000] and add a small amount (7–10 mL/min) of ammonia gas to the spray chamber in order to ensure the environment is basic and boron is not present as the volatile boric acid species. Using this method, a 20 ppb boron solution can be washed out to ~1% within 1 min, and a precision on the B/Ca ratio of 3% (2 SD) is readily achievable. The other trace element ratios (with the exception of Al/Ca) are not significantly affected by this modification to sample introduction [*Ni*, 2006]. However, the Al/Ca ratio is often lower in samples run with ammonia, perhaps because of the formation of an Al-rich secondary precipitate within the spray chamber.

[11] The accuracy of the B/Ca ratio measured in this way has been determined by cross-calibration of samples by isotope dilution, using the ^{10}B enriched NIST SRM 952 boric acid and TIMS isotopic measurements. These boron concentrations have then been converted to B/Ca ratios by determining calcium concentrations in two ways: first, by accurate measurements of sample weights assuming the samples are pure $CaCO_3$, and, second, by ^{43}Ca intensity measurements on the Element 2 ICPMS relative to gravimetric standards. As shown in Table 2, these two methods agree well (from 0.6 to 5.4%) and we adopt a conservative estimate of our B/Ca accuracy of 5%.

3. Background

3.1. Isotopic and Elemental Proxies

[12] In seawater, boron has two dominant species, boric acid $B(OH)_3$ and borate ion $B(OH)_4^-$ (Figure 1a). There is a pronounced isotopic fractionation between the species [*Kakihana et al.*, 1977] (see also Figure 1b), although the exact value of the fractionation is currently a subject of some debate [*Pagani et al.*, 2005; *Zeebe*, 2005; *Tossell*, 2005; *Liu and Tossell*, 2005; *Klochko et al.*, 2006]. Since the proportion of a given boron species is pH dependent, the isotopic composition of the species is also strongly pH dependent (Figure 1). *Hemming and Hanson* [1992] found that boron is incorporated into biogenic and inorganic marine calcium carbonates predominantly as the charged $B(OH)_4^-$ species. Thus the isotopic composition of carbonate is highly sensitive to variations in pH, e.g., ~1‰ change in $\delta^{11}B$ for every 0.1 pH units at typical seawater pH. This forms the basis of boron isotope pH proxy [e.g., *Vengosh et al.*, 1989; *Hemming and Hanson*, 1992; *Spivack et al.*, 1993; *Sanyal et al.*, 1995; *Palmer et al.*, 1998; *Hönisch and Hemming*, 2005] the theory for which is expounded in greater detail elsewhere [see *Zeebe and Wolf-Gladrow*, 2001; *Pagani et al.*, 2005].

[13] This pH-dependent speciation of boron also forms the basis of a potential B/Ca proxy for the ocean carbonate system, which has so far been little explored. The boron concentration of carbonate reflects the pH of the solution from which it grew [*Hemming and Hanson*, 1992; *Sanyal et al.*, 1996, 2000] because the availability of the incorporated $B(OH)_4^-$ species is moderated by solution pH (Figure 1). The exchange distribution coefficient, Kd, for B substitution into calcium carbonate can be expressed as:

$$\mathrm{Kd} = \left[\mathrm{HBO_3^{2-}}/\mathrm{CO_3^{2-}}\right]_{\mathrm{solid}} / \left[\mathrm{B(OH)_4^-}/\mathrm{HCO_3^-}\right]_{\mathrm{fluid}} = [\mathrm{B/Ca}]_{\mathrm{solid}} / \left[\mathrm{B(OH)_4^-}/\mathrm{HCO_3^-}\right]_{\mathrm{fluid}} \quad (1)$$

where square brackets indicate molar concentrations (although strictly speaking they should be activities).

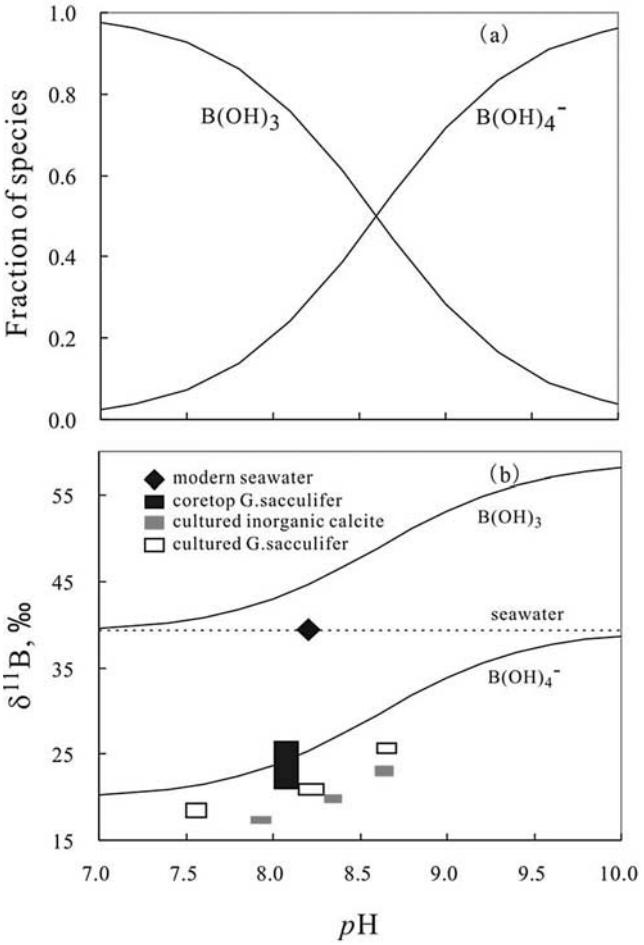

Figure 1. (a) Distribution of aqueous boron species versus pH calculated from K values listed by *Zeebe and Wolf-Gladrow* [2001] (pK* = 8.6 at T = 25°C, S = 35, and P = 0 bar). (b) The δ^{11}B of the two dominant aqueous species of boron versus pH calculated from the fractionation factor of *Kakihana et al.* [1977] (K = 1.01935 at T = 25°C, and S = 35). Also plotted is seawater (diamond) and core top *G. sacculifer*, cultured *G. sacculifer*, and inorganic calcite from *Hemming and Hanson* [1992], *Palmer and Pearson* [2003], *Hönisch and Hemming* [2004], *Foster et al.* [2006], *Sanyal et al.* [2001], and this study.

[14] *Zeebe and Wolf-Gladrow* [2001] calculated an average boron distribution coefficient from the data of *Hemming and Hanson* [1992] of 0.012, in a sample set containing aragonitic corals and high-Mg marine carbonates, but no foraminifers. At typical seawater pH, an increase of 0.1 pH units equates to ~25% increase in boron concentration in foraminiferal calcite, regardless of the absolute Kd. Given measurement precision of B/Ca in calcite better than 5% (see above), this large change provides the potential for a very sensitive proxy for the carbonate system in the past. Moreover, the dependence of the boron concentration in calcite on the ratio of $[B(OH)_4^-]/[HCO_3^-]$ in seawater offers a method of calculating the $[HCO_3^-]$ of seawater given a knowledge of the $[B(OH)_4^-]$ which can be calculated from boron isotope measurements. A tandem measurement of B concentration and isotopic composition potentially allows the oceanic carbonate system to be fully constrained, and hence paleo-pCO_2 can be calculated without additional assumptions [cf. *Hönisch and Hemming*, 2005]. However, there is a need to calibrate the B/Ca Kd for different foraminiferal species and this has been the important goal of recent work by *Yu et al.* [2007]. They have calibrated B/Ca using core top *Globorotalia inflata* and *Globigerina bulloides*, and performed a down core calibration of *G. ruber*. Their principal findings indicate that B/Ca in foraminifers reflects both pH and sea surface temperature (in addition to the temperature effects on speciation of carbonate and boron). Importantly for this study, they also show markedly different absolute K_d for different species.

[15] U/Ca ratios in foraminifers also have recently been suggested as a possible proxy to constrain the oceanic carbonate system. Culture studies demonstrated a tight correlation between U/Ca in foraminiferal calcite and seawater $[CO_3^{2-}]$ which has been largely interpreted as a result of the formation of highly stable complexes between uranyl ion $[UO_2^{2+}]$ and $[CO_3^{2-}]$ [e.g., *Russell et al.*, 2004]. *Russell et al.* [1996] previously found that U/Ca ratios of the glacial planktic foraminifers (*G. sacculifer* and *G. ruber*) from the Caribbean and the eastern equatorial Atlantic oceans were ~25% lower than Holocene ones and the authors explained this change as a consequence of variations in seawater $[CO_3^{2-}]$, or temperature. Culture experiments of *O. universa* showed that U/Ca decreases by 25 ±7% per 100 μmol kg^{-1} increase in $[CO_3^{2-}]$ and that between 15°C and 25°C U/Ca is insensitive to temperature [*Russell et al.*, 2004].

[16] The trace element analysis routine used in this study also determines other trace element abundances, relative to Ca, employed as paleoceanographic proxies, notably Mg/Ca, Li/Ca and Sr/Ca. Therefore we can assess the behavior of these proxies in tandem with tracers of the ocean carbonate system. Mg/Ca ratios in planktic foraminifers are well known to be predominantly controlled by temperature [e.g., *Nürnberg et al.*, 1996; *Anand et al.*, 2003]. Both culture experiments and field studies (core top samples and sediment traps) have demonstrated an exponential relationship between Mg/Ca ratios and calcification temperature [e.g., *Dekens et al.*, 2002; *Anand et al.*, 2003]. However, the relationship between foraminiferal Mg/Ca and ambient temperature is species and site dependent which might indicate influences of secondary factors. For instance, is has been suggested that Mg/Ca ratios may be affected by calcification rate [*Elderfield et al.*, 2002]. Higher ambient carbonate ion concentration leads to heavier tests in several species [*Bijma et al.*, 1999, 2002; *Barker and Elderfield*, 2002], an observation which points toward differences in calcification rate. It should be noted however that since we do not know the duration of individual chamber formation, we can only refer here and throughout to an increase in overall calcification rate. Nonetheless, it might be expected that there would be a relationship between B isotope ratio and Mg/Ca variability, which we can examine in this study.

[17] Culture experiments reveal that Sr/Ca ratios in foraminiferal calcite reflect both seawater Sr/Ca and temperature but salinity exerts only a small influence on the Sr

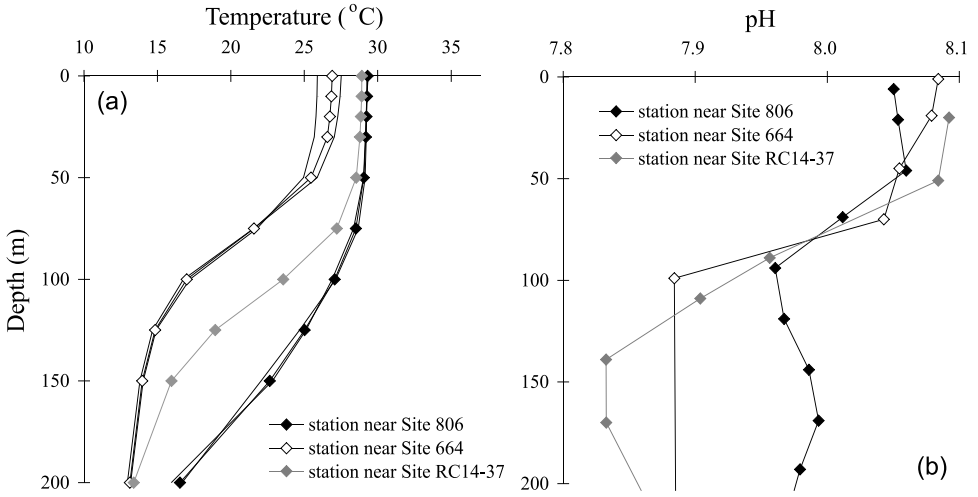

Figure 2. (a) Modern mean annual seawater temperature-depth profile of stations nearest to the sites of interest from the World Ocean Analysis 2005 data set. The mixed layer is ~70 m at both the Pacific and Indian sites (Site 806 and Site RC14-37, respectively), and ~40 m at the Atlantic site (Site 664) (R. Schlitzer, Ocean Data View, 2000, available a http://www.awi-bremerhaven.de/GEO/ODV). Also shown for the stations near Sites 664 and 806, as an indicator of seasonal variation, are the average summer and winter season temperatures from the World Ocean Analysis data set. (b) Modern seawater pH-depth profile for the nearest stations from the World Ocean Circulation Experiment (WOCE) data set (R. Schlitzer, Ocean Data View, 2000). Note that in the mixed layer pH shows no significant change.

partition coefficient [*Delaney et al.*, 1985; *Lea et al.*, 1999]. Li/Ca ratios in foraminiferal calcite have received less attention but have been inferred to be dependent upon seawater [CO_3^{2-}] by *Hall and Chan* [2004] and are inversely correlated with temperature [*Marriott et al.*, 2004a, 2004b]. Again, the tandem analysis of boron isotope ratio with Li/Ca ratio allows an assessment of the sensitivity of this ratio to the ocean carbonate system.

3.2. Ecology of *G. sacculifer and G. ruber*

[18] In order to interpret correctly the trace element and boron isotopic data it is instructive to review the ecology of the two species (*G. ruber* and *G. sacculifer*) we have chosen to study. *G. ruber* is a symbiont bearing species with dinoflagellate symbionts living in the mixed layer, mainly above 25 m [*Hemleben et al.*, 1989], where most environmental parameters are roughly constant (Figure 2). Plankton tow samples from the equatorial Atlantic near Site 664C corroborate this habitat depth [*Kemle-von Mücke and Oberhänsli*, 1999]. *G. ruber* does not deposit a gametogenic crust of any significant thickness [*Caron et al.*, 1990] and hence has relatively homogenous Mg/Ca and $\delta^{18}O$ within its test [*Eggins et al.*, 2003; *Benway et al.*, 2003].

[19] *G. sacculifer* also bears dinoflagellate symbionts and inhabits the mixed layer [*Hemleben et al.*, 1989]. In areas with a thick mixed layer, *G. sacculifer* tends to live in water deeper than *G. ruber*, whereas in areas with a very shallow thermocline (such as the equatorial Atlantic, Figure 2) *G. sacculifer* and *G. ruber* live at the same water depth [*Kemle-von Mücke and Oberhänsli*, 1999]. The principal difference between the two species is that *G. sacculifer* covers its test with a significant amount of gametogenic calcite crust during gametogenesis (~30%; [*Bé*, 1980]) which oxygen isotope analyses suggest occurs at the pycnocline [*Schmidt and Mulitza*, 2002]. Laser ablation ICPMS Mg/Ca analyses through the tests of *G. sacculifer* show that these final calcification deposits have lower Mg/Ca ratios, which has been interpreted as reflecting lower temperatures (2°–3°C) and deeper habitat depths [*Eggins et al.*, 2003] but may also result from a different calcification mechanism [*Erez*, 2003]. It is the migration of *G. sacculifer* out of the mixed layer during ontogeny and the subsequent deposition of significant amounts of gametogenic calcite at depth where environmental parameters are different (Figure 2) that is the most relevant variation between these two species for this particular study.

4. Results

4.1. The $\delta^{11}B$ Variation With Test Size

[20] In *G. sacculifer* from the Pacific and Indian oceans, $\delta^{11}B$ increases with increasing test size reaching a plateau at sizes larger than 460 μm (Figure 3 and Table 3). Our data from the Indian Ocean site show a similar pattern to analyses of the same samples by *Hönisch and Hemming* [2004], but are offset by ~3‰ toward heavier $\delta^{11}B$ (see section 2). Likewise, our samples from the Pacific show a similar trend but again with a ~3‰ offset to the Pacific samples from a nearby core analyzed by *Hönisch and Hemming* [2004]. In contrast, there is no discernable variation in the $\delta^{11}B$ of *G. sacculifer* in the Atlantic site and the average $\delta^{11}B$ of all sizes is 23.7 ± 0.7‰ (2 SD). There is no systematic variation of $\delta^{11}B$ with test size for *G. ruber* in either Atlantic or Pacific site. The average for all *G. ruber* is very similar to that of Atlantic *G. sacculifer* at $\delta^{11}B$ of 23.1 ± 0.8‰ (Figure 3).

4.2. Trace Elemental Abundance Variations With Test Size

[21] Trace elemental abundances, expressed as molar ratios relative to stoichiometrically controlled calcium, are

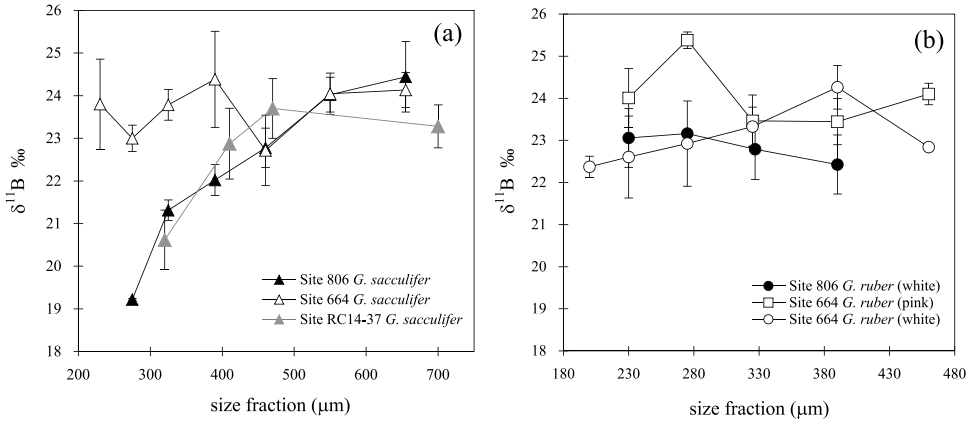

Figure 3. (a) The δ^{11}B versus size fraction for *G. sacculifer* with final sac-like chamber in Pacific Site 806, Atlantic Site 664, and Indian Site RC14-37. (b) The δ^{11}B versus size fractions in *G. ruber* (white and pink) in Pacific Site 806 and Atlantic Site 664. In Figures 3a and 3b, error bars are the 2 standard error uncertainties of repeat measurements.

reported in Table 3 and Figures 4 and 5. These data, determined on the same samples analyzed for boron isotopes, show notable variations with test size.

[22] U/Ca increases dramatically with increasing test size in both *G. sacculifer* and *G. ruber*. For *G. sacculifer*, the change in U/Ca between largest and smallest size fractions analyzed is ~60% at Site 806B and ~45% at Site 664C (Figures 4a and 4b). B/Ca ratios also show clear size dependence in both *G. sacculifer* and *G. ruber*, but with a constant offset between Pacific and Atlantic sites for *G. sacculifer* (Figures 4c and 4d). Similarly Li/Ca ratios increase with increasing size fraction in both species but the ~10% change is closer to analytical uncertainty and consequently there is more scatter in these ratios (Figures 4e and 4f).

[23] Mg/Ca increases with increasing size fraction in *G. sacculifer* in both Atlantic and Pacific sites by 17% and 13% respectively (Figures 5a and 5b), but the variability of Mg/Ca ratio in *G. ruber* is much smaller and closer to our reproducibility for repeat dissolutions (2%; 2 SD). In contrast to the other trace elemental abundances, Sr/Ca values decrease with increasing size, although the total range of Sr/Ca is again close to our analytical resolution (Figures 5c and 5d). These trends in Mg/Ca and Sr/Ca are similar in magnitude and direction to other studies of this kind [e.g., *Elderfield et al.*, 2002].

5. Discussion

[24] In the following discussion we use the environmental differences between our sample sites (Figure 2) and the principal biological differences between the two species (i.e., absence/presence of gametogenic carbonate and the slightly different habitat depth) to explore their effect on the measured δ^{11}B for each species and their influence on trace element incorporation into foraminiferal carbonate.

5.1. Influences of Partial Dissolution on δ^{11}B

[25] *Hönisch and Hemming* [2004] noted, as we do here, that δ^{11}B in *G. sacculifer* increases with increasing size fraction in both the Indian and Pacific oceans. They concluded that this isotopic variation is predominantly due to the microenvironmental pH control caused by symbiont photosynthesis, calcification and respiration, following the model of *Zeebe et al.* [2003]. This explanation however cannot account for our new data on Atlantic *G. sacculifer* (Figure 3) which shows no significant size related δ^{11}B variation. Likewise the symbiont bearing *G. ruber* shows no comparable variation in either core (Figure 3).

[26] Isotopic fractionations of boron are unlikely to be caused by variations in calcification rate because of the very rapid isotopic equilibration time [*Zeebe et al.*, 2001]. Furthermore, large changes in the process of calcification are unlikely to occur at similar environmental settings in the different ocean basins. Hence kinetic isotopic fractionations do not readily explain the difference between Pacific and Atlantic *G. sacculifer* specimens.

[27] One important difference between our sites is the carbonate saturation state (Ω) of the deepwater. Using oceanographic data (temperature, salinity, alkalinity and total dissolved inorganic carbon) from nearby World Ocean Circulation Experiment (WOCE) stations (6078B, 22015B and 24442B (R. Schlitzer, Ocean Data View, 2000, available at http://www.awi-bremerhaven.de/GEO/ODV)), we calculate that bottom water is saturated with respect to calcite ($\Omega > 1$) at all sites but becomes increasingly less supersaturated from Atlantic to Pacific sites ($\Omega = 1.13$ for Site 806B at 2560m, $\Omega = 1.17$ for Site RC14-37PC at 2230m, and $\Omega = 1.22$ for Site 664C at 3600m; where Ω is calculated using constants of *Zeebe and Wolf-Gladrow* [2001]). Likewise, all sites lie above the lysocline (inferred from foraminiferal preservation indices and bulk sediment carbonate content [*Berger et al.*, 1982; *Peterson and Prell*, 1985]). Foraminiferal crystallinity, a quantitative preservation index [*Bassinot et al.*, 2004], shows that even at shallow depths on the Ontong Java Plateau, forams are less well preserved than those from the equatorial Atlantic at water depths greater than that of Site 664C. Furthermore, dissolution of *G. ruber* can be demonstrated on the Ontong Java Plateau above the lysocline in samples from ~2800 m water depth [*Bonneau et al.*, 1980; *Kimoto et al.*, 2003].

Table 3. The $\delta^{11}B$ and Metal/Ca Ratios Versus Size Fractions in the Surface and Deep Dwelling Species

Size, um	Mg/Ca, mmol/mol	Sr/Ca, mmol/mol	Mn/Ca, μmol/mol	Cd/Ca, μmol/mol	Ba/Ca, μmol/mol	U/Ca, nmol/mol	Li/Ca, μmol/mol	Na/Ca, mmol/mol	Al/Ca, μmol/mol	Nd/Ca, μmol/mol	B/Ca, μmol/mol	$\delta^{11}B$,[a] ‰	2 SE	n[b]
ODP Site 806, Pacific 1H-1, 12–17 cm, G. sacculifer[c]														
600–710	4.23	1.28	33.56	0.17	1.18	14.62	7.34	5.14	15.88	0.48	74.94	24.4	0.8	7
500–600	4.39	1.29	38.28	0.41	1.81	14.42	0.00	5.17	14.39	0.52	75.20	24.0	0.4	3
425–500	4.24	1.30	28.04	0.15	1.27	12.09	7.76	5.19	3.63	0.58	69.67	22.8	0.5	3
355–425	4.25	1.29	42.09	0.28	1.37	10.52	10.31	5.23	22.63	0.71		22.0	0.4	2
300–355	3.94	1.29	24.40	0.17	1.24	8.64	9.82	5.07	45.07	0.67	66.50	21.3	0.2	3
250–300	3.70	1.32	30.92	0.16	1.01	7.70	7.05	5.14	7.88	0.48		19.2	0.0	2
ODP Site 806, Pacific 1H-1, 12–17 cm, G. ruber (white)														
355–425	4.40	1.41	32.54	0.25	1.16	10.65	14.14	6.13	30.58	1.07		22.4	0.7	2
300–355	4.42	1.40	41.97	0.23	1.82	9.77	14.09	6.46	18.17	0.86	111.69	22.8	0.7	3
250–300	4.46	1.43	47.53	0.21	2.03	9.33	13.07	5.96	33.18	0.67	110.68	23.2	0.0	2
212–250	4.56	1.42	32.38	0.25	1.32	8.26	12.72	5.85	14.17	0.50	101.35	23.1	0.7	1
ODP site 664, Atlantic, 1H-1, 10–12 cm, G. sacculifer[c]														
600–710	3.63	1.27	20.89	0.14	1.37	10.84	13.95	6.36	21.27	0.94	97.08	24.1	0.4	3
500–600	3.70	1.29	28.55	0.13	1.42	11.98	13.02	5.91	38.32	0.82		24.0	0.5	3
425–500	3.60	1.30	21.71	0.12	1.56	10.86	13.25	6.06	33.91	0.80	86.97	22.7	0.8	4
355–425	3.47	1.31	9.68	0.13	1.15	8.98	12.44	5.89	12.14	0.69	86.46	24.4	1.1	3
300–355	3.30	1.33	15.79	0.13	1.32	8.00	12.26	6.28	22.50	0.86	86.97	23.8	0.4	3
250–300	3.24	1.32	15.03	0.13	1.40	7.70	12.70	6.25	14.95	0.79	79.34	23.0	0.3	3
212–250	3.20	1.33	17.86	0.13	1.29	6.74	12.12	5.98	18.50	0.69	84.56	23.8	1.1	3
ODP site 664, Atlantic, 1H-1, 10–12 cm, G. ruber (pink)														
425–500	3.632	1.38	37.72	0.15	2.57	13.47	16.31	6.53	72.28	0.92	125.43	24.1	0.3	3
355–425	3.525	1.39	20.00	0.14	1.44	13.31	15.34	6.54	32.12	0.91	119.08	23.4	0.5	4
300–355	3.582	1.38	23.94	0.14	1.76	11.08	15.75	6.47	44.15	0.81	110.43	23.5	0.6	2
250–300	3.560	1.41	13.62	0.14	1.42	11.33	14.33	6.32	20.42	0.83		25.4	0.2	2
212–250	3.465	1.39	20.53	0.14	1.66	9.30	15.21	6.48	40.20	0.79	94.66	24.0	0.7	2
ODP site 664, Atlantic, 1H-1, 10–12 cm, G. ruber (white)														
425–500	3.68	1.37	10.67	0.20	3.06	13.93	15.88	7.55	86.45	1.14		22.8	0.1	2
355–425	3.87	1.37	19.96	0.17	1.53	9.75	16.76	7.25	22.38	0.76	116.41	24.3	0.5	6
300–355	3.87	1.39	25.38	0.13	1.79	9.70	15.30	6.33	51.75	0.82	113.44	23.3	0.5	2
250–300	4.00	1.39	14.25	0.15	1.23	9.78	13.49	6.35	27.73	0.88	65.89	22.9	1.0	2
212–250	3.94	1.37	25.50	0.13	1.58	8.12	15.04	6.40	35.40	0.81	117.31	22.6	1.0	2
180–212	4.08	1.40	32.65	0.14	1.89	7.91	14.92	6.45	38.07	0.86	107.42	22.4	0.3	2
RC 14-37 PC, Indian Ocean, 1H-1, 0–4 cm, G. sacculifer[c]														
515–865												23.3	0.5	2
425–515												23.7	0.7	1
380–425												22.9	0.8	2
250–350												20.6	0.7	1

[a]Permil deviation from NIST SRM 951, $^{11}B/^{10}B_{TE} = 4.0396$.
[b]Number of repeat measurements denoted by n, where n = 1 the 2 SE is assumed to be 0.7‰.
[c]With final sac-like chamber.

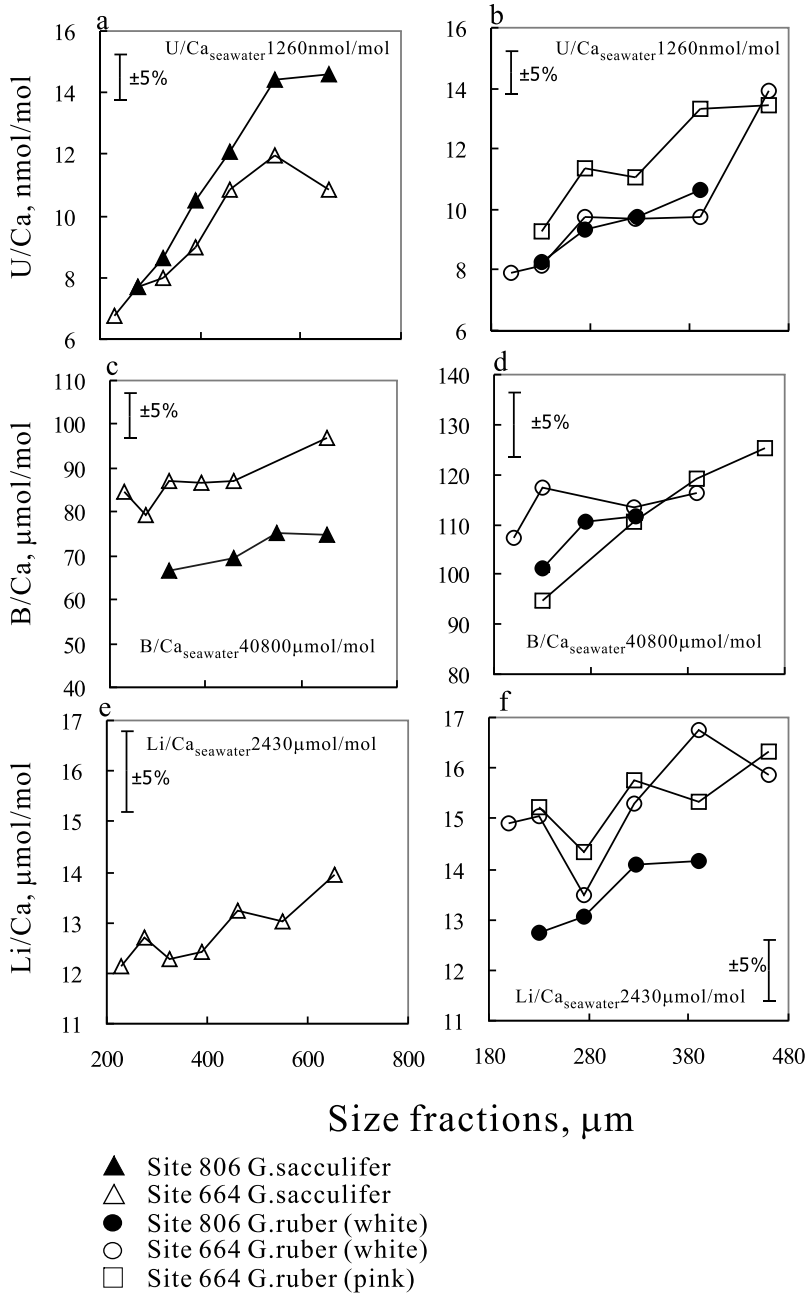

Figure 4. (a and b) U/Ca, (c and d) B/Ca, and (e and f) Li/Ca ratios versus size fraction for both *G. sacculifer* and *G. ruber* (white and pink) in Pacific Site 806 and Atlantic Site 664. Also shown are the relevant seawater metal/Ca ratios.

[28] Notably, dissolution will affect *G. ruber* more than *G. sacculifer* in terms of relative mass loss [*Hemleben et al.*, 1989]. The contrasting behavior of $\delta^{11}B$ in the two species from the Pacific sample cannot simply result from isotopic fractionation through dissolution but instead plausibly involves the preferential dissolution of an isotopically heterogeneous *G. sacculifer* test. Gametogenic calcite represents up to 30% of the calcite of *G. sacculifer* while *G. ruber* has almost no gametogenic calcite [*Bè*, 1980]. Thus we suggest preferential dissolution of ontogenetic relative to gametogenic calcite in *G. sacculifer* is responsible for the differences in boron isotopic compositions observed in Figure 3.

[29] Micro-pH measurements in the immediate vicinity of *G. sacculifer* indicate that the pH of the seawater surrounding this species is significantly modified by the life processes of the foraminifer and its photosynthesizing symbionts [*Rink et al.*, 1998; *Wolf-Gladrow et al.*, 1999]. The pH in the microenvironment of a foraminifer is controlled by calcification and respiration, which both decrease pH, and photosynthesis of the symbionts which increases pH. The boron isotopic composition of the test

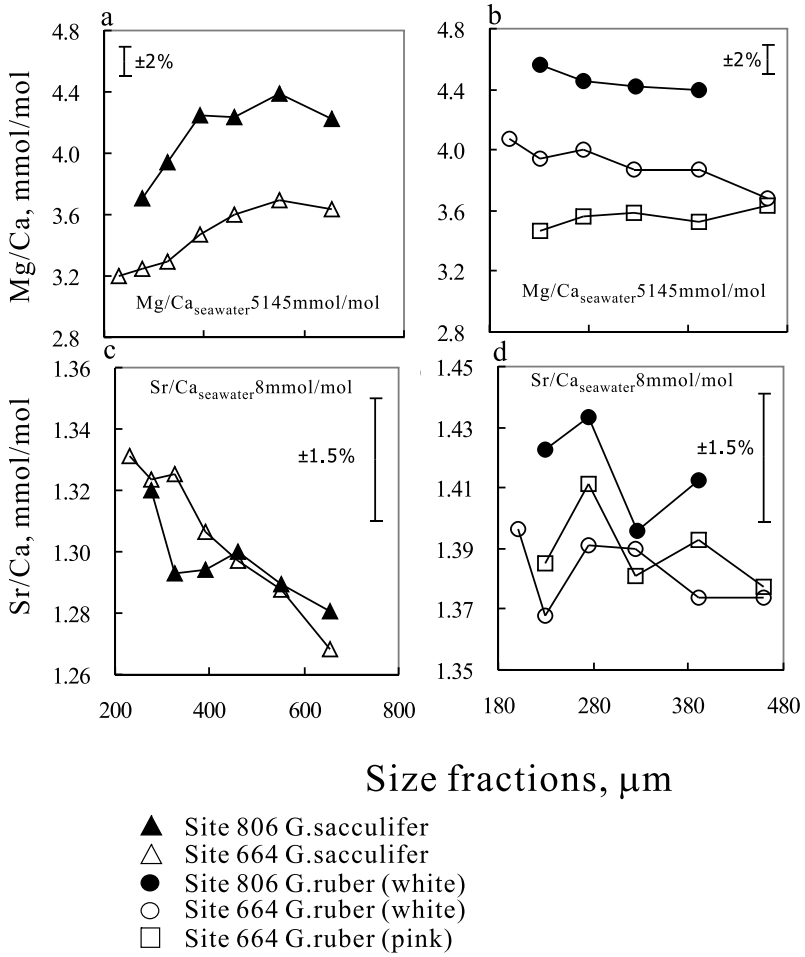

Figure 5. (a and b) Mg/Ca and (c and d) Sr/Ca ratios versus size fraction in both *G. sacculifer* (with final sac-like chamber) and *G. ruber* (white and pink) in Pacific Site 806 and Atlantic Site 664. Also shown are the relevant seawater metal/Ca ratios.

therefore should depend on the relative importance of these processes. The larger the foraminifer the more symbionts it harbors [*Spero and Parker*, 1985; *Spero et al.*, 1991] and hence the larger their potential influence. On the other hand, light levels decrease with water depth and hence depth migration also influences the exposure of the symbionts to light. Indeed, *Hönisch et al.* [2003] demonstrated that under low-light conditions (and correspondingly reduced photosynthetic rates) the boron isotopic compositions of the tests of *O. universa* are 1.5‰ lighter than tests grown under high-light levels (and consequently elevated photosynthetic rates). The symbionts are expelled or digested before gametogenic calcification begins [*Bé et al.*, 1985]. This loss of photosynthesis (and hence uptake of CO_2 by the dinoflagellates) decreases the local pH and δ^{11}B. Consequently the gametogenic crust will be isotopically lighter than the ontogenetic calcite grown closer to the surface with active photosynthesis by the symbiont. Moreover, *G. sacculifer* sinks to the top of the thermocline before undergoing gametogenesis [*Schmidt and Mulitza*, 2002] and so changes in ambient water column chemistry may further promote light δ^{11}B in its gametogenic calcite (Figure 6). Gametogenic calcite is more dissolution resistant than ontogenetic calcite [*Hemleben et al.*, 1989; *Erez*, 2003]. Thus partial dissolution of *G. sacculifer* will change the ratio between ontogentic calcite grown at the surface at high light levels with a relatively heavy δ^{11}B and the gametogenic calcite grown at depth without symbitons with an isotopically light isotopic ratio (see Figure 6).

[30] Furthermore, it has been observed that small foraminifers are more affected by dissolution than larger individuals as a result of their higher surface area to volume ratio [*Berger and Piper*, 1972; *Berger et al.*, 1982]. Consequently, smaller *G. sacculifer* will be relatively more enriched in gametogenic calcite than larger individuals after partial dissolution. *Hönisch and Hemming* [2004] make a similar argument for their Pacific *G. sacculifer* recovered from greater depth. The lack of a size variation in our Atlantic *G. sacculifer* samples is therefore consistent with the better preservation potential at site 664C. The absence of size related changes in δ^{11}B in *G. ruber* in the more poorly preserved Pacific core can be explained by the lack of a gametogenic layer in this species [*Caron et al.*, 1990]. Thus

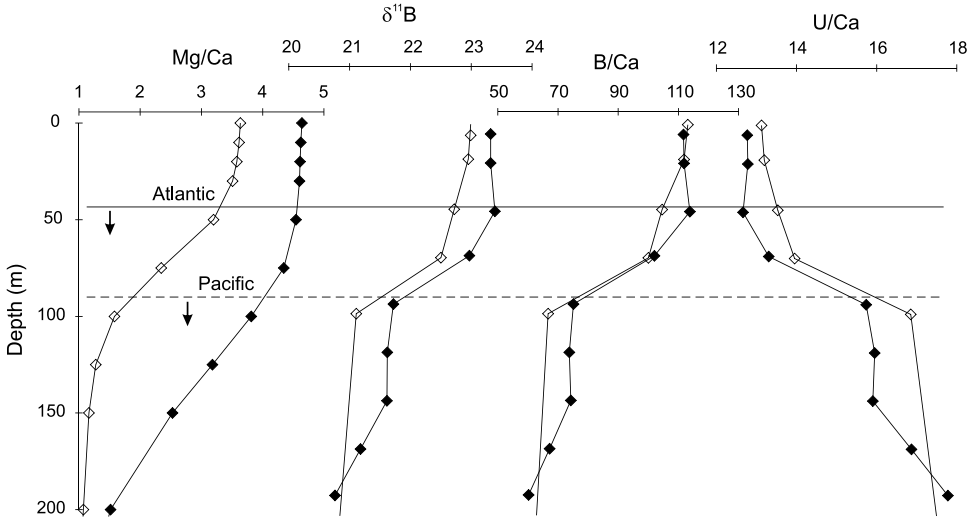

Figure 6. Predicted variation in Mg/Ca, δ^{11}B, B/Ca, and U/Ca with depth in foraminifera from sites 664 (open diamonds) and 806 (solid diamonds). These predictions are made using the seawater analyses from the WOCE and World Ocean Analysis data sets (same data as in Figure 2) and the empirical relationships described in the literature between Mg/Ca in foraminifera and temperature [*Anand et al.*, 2003] and U/Ca and [CO_3^{2-}] (described by *Russell et al.* [2004] for the *G. bulloides* species). For δ^{11}B, carbonate values were determined following the approach of *Hönisch and Hemming* [2005], and for B/Ca we assumed a Kd = 0.00142 and used the equations described in the text. This Kd was chosen because it is the Kd calculated at Site 664 for *G. ruber*. For the reconstructions of the Holocene carbonate system required to predict U/Ca, B/Ca, and δ^{11}B, we used modern alkalinity as measured by WOCE and calculated a preindustrial $[CO_2]_{aq}$ assuming equilibrium with the preindustrial atmosphere, an assumption that is likely to be valid at these sites [see *Takahashi et al.*, 2002]. The calculated acidification was then applied to the upper 200 m of the water column. This is clearly an oversimplification but does not unduly compromise the significance of these plots. Depths where the temperature is more than 1°C colder than the mixed layer lie below the horizontal line (dashed for Pacific and solid for Atlantic). We propose that *G. sacculifer* sinks to below these depths to deposit its gametogenic calcite, which results in a larger compositional difference between ontogenic and gametogenic calcite in the Pacific site compared to Atlantic site (see text).

we suggest that *G. ruber* is the most reliable species for paleo-pH analysis.

5.2. Trace Elemental Abundances

[31] In the past two decades, a series of studies have concentrated on trace elemental abundances in foraminifers as proxies for a number of ocean properties (e.g., see review by *Henderson* [2002]). Despite numerous efforts to investigate the controls on trace element incorporation into foraminiferal carbonate, the exact processes remain uncertain. A number of authors have suggested that [CO_3^{2-}] has a major or modifying influence on some trace elemental abundances in foraminiferal calcite [e.g., *Elderfield et al.*, 2002; *Dekens et al.*, 2002; *Russell et al.*, 2004; *Hall and Chan*, 2004]. Our combined measurements of δ^{11}B and trace elements allow us to assess the link between [CO_3^{2-}] and trace element incorporation.

[32] As discussed earlier, B/Ca and U/Ca (and Li/Ca) ratios have been suggested as proxies for various parameters of the oceanic carbonate system. The contrast between the highly variable B/Ca and U/Ca ratios (Figure 4) compared to the largely invariant δ^{11}B (Figure 3) is thus puzzling. For example, U/Ca ratios in *G. ruber* decrease by ~25% from biggest test to the smallest size fraction. Using the calibration of *Russell et al.* [2004] this equates to an increase in [CO_3^{2-}] of ~100 μmol/kg. Our data for *G. ruber* do not show a corresponding size-dependent δ^{11}B difference of ~2‰ (Figure 3b). Similarly, if the 32% shift in B/Ca shown by *G. ruber* (pink) at Site 664C were driven by pH, this should result in an associated change of ~2.5‰ in δ^{11}B, but again this is also not observed. What is more, if the changes in B/Ca and U/Ca were driven solely by the carbonate system they should be negatively correlated (e.g., see Figure 6), which is clearly not the case (Figure 4).

[33] The increases in B/Ca, U/Ca (and also Li/Ca) with increasing size for both species at both sites suggests a control by the processes of calcification rather than a species or local effect. During calcification, ions cross the cell membrane through selective channels, for example, the Ca^{2+} ions are transported from the seawater through the Ca^{2+}-selective channels into the cytosol [*Erez*, 2003]. This can explain significantly lower concentrations of all the measured cationic species relative to Ca in calcite compared to seawater (Figure 4). As *Rickaby et al.* [2002] proposed for coccolithophores, foraminifers may be able to control the efficiency of these calcite channels better at low calci-

fication rates, and hence more efficiently discriminate against incorporation of trace elements into the calcite lattice. At high calcification rates the discrimination becomes less efficient resulting in more similar trace metal/calcium ratio to seawater which for B, U and Li is considerably higher than is found in foraminiferal carbonate (Figure 4).

[34] Large individuals grow, on average, faster than the small ones during their life span [*Schmidt et al.*, 2004] and hence they plausibly calcified faster [*Anderson and Faber*, 1984]. *Anderson and Faber* [1984] estimated mean hourly rates of calcification in *G. sacculifer* of 53×10^{-2} μg per chamber per hour for organisms with a final size of 623 μm and 87×10^{-2} μg per chamber per hour for organisms with a final size of 730 μm. This is in contrast to the suggestion of *Elderfield et al.* [2002], who argued that smaller individuals contain a larger proportion of a fast calcifying, early growth phase. Although we favor changes in calcification rate as a possible control on the evident differences in trace element abundances with different test size, there are several other mechanisms that may also operate in tandem with apparent calcification rate but are more difficult to distinguish.

[35] Further subtleties in the relationship between B/Ca, U/Ca and test size require discussion and mitigate against a simple, entirely self-consistent interpretation of all chemical parameters described above. Using the ambient temperature, salinity and preindustrial carbonate system parameters at the Pacific and Atlantic sites allows us to calculate that the B/Ca Kd for *G. ruber* at both sites is similar being around 0.0014 to 0.0015. Notably, these estimates are very similar to the B/Ca Kd of *Yu et al.* [2007] for *G. ruber* from the equatorial Atlantic. However, in a comprehensive core top calibration of B/Ca in the Atlantic for several species (notably not including *G. ruber*) *Yu et al.* [2007] find that the B/Ca Kd is temperature dependent (in addition to the temperature effect on the carbonate system parameters and boron speciation). However, our limited data set for *G. ruber* does not show such a relationship, most likely because of the limited range of temperatures investigated here ($\sim$3°C).

[36] The B/Ca of *G. sacculifer* are systematically lower than *G. ruber*, in keeping with strong species differences observed by *Yu et al.* [2007]. Moreover, the B/Ca ratios of *G. sacculifer* from the Pacific core (ODP Site 806) are systematically lower than the Atlantic samples (ODP Site 664). This difference likely stems from the environmental differences highlighted in Figure 6. As is evident in Figure 6, the predicted B/Ca at the upper regions of the thermocline of Site 806 is lower than at Site 664. Thus the gametogenic calcite and consequently the bulk tests of our Pacific *G. sacculifer* should have lower B/Ca than our Atlantic samples (see Figure 4). The lack of similar contrast between δ^{11}B between our Pacific and Atlantic *G. sacculifer* (Figure 3) perhaps reflects the lower sensitivity of δ^{11}B to these changes in water column chemistry (Figure 6). However, it is puzzling that the influence of partial dissolution of Pacific *G. sacculifer*, which results in such a marked test size dependence in δ^{11}B for samples from this site, is not equally evident in B/Ca. This suggests the influence of additional factors, notably *Schmidt and Kasemann* [2006] presented analyses by Secondary Ion Mass Spectrometry of anomalously heavy δ^{11}B in foraminiferal proloculi and juvenile parts of the test, which, if preferentially dissolved, could cause a change in the bulk δ^{11}B of the tests. Clearly further work is required to mesh all these observations. The implication of this study is nonetheless that the depth migration and ontogeny of *G. sacculifer* (and other foraminifer) is likely to generate heterogeneities within the test that may lead to fractionations in δ^{11}B and B/Ca following dissolution. The magnitude of these intertest variations probably varies from site to site with changing environmental parameters (Figure 6).

[37] In keeping with the discussion above, the lower ambient pH and $[CO_3^{2-}]$ of deeper grown gametogenic calcite in Pacific *G. sacculifer* can also account for the higher U/Ca of the Site 806 samples (Figure 4). Furthermore, the greater relative change of U/Ca of the Pacific *G. sacculifer* with decreasing test size is indicative of the influence of preferential dissolution of the higher U/Ca ontogenic calcite, as invoked to account for the δ^{11}B variability in these samples.

[38] Although Li/Ca ratios have been argued to reflect differences in $[CO_3^{2-}]$, our data suggest a much stronger influence of temperature. There appears to be a systematic difference between *G. ruber* from the Pacific and Atlantic, with lower values in the Pacific. Using the relationship of *Marriott et al.* [2004a] the temperature difference between these sites should result in 12% difference in the Li/Ca, which is similar to our data. This result is also in keeping with the more commonly used Mg/Ca ratios (Figure 5).

[39] While overall growth rates during the life of the organisms can potentially explain the general increase in U/Ca, B/Ca and Li/Ca ratios with increasing size in both foraminiferal species, this mechanism does not explain Mg/Ca changes, since the Mg/Ca ratio only shows a size correlation in *G. sacculifer*. We therefore suggest that the growth rate of the organism does not affect the incorporation of Mg. This interpretation is consistent with culture experiments of *Segev and Erez* [2006] who noted that calcium carbonate Mg concentration in biogenic calcite is not correlated with the rate of calcification. This observation is in stark contrast with inorganic precipitation experiments which display a dependence of the D_{Mg} of inorganic calcite on precipitation kinetics. Similarly, *Cutani* [1984] and *Erez* [2003] determined a decrease of D_{Sr} with increasing calcification rates for foraminifers in contrast to the result of the inorganic precipitation experiments [*Rickaby et al.*, 2002]. This "biological" decrease of D_{sr} is consistent with our observations of a small decrease of Sr/Ca ratio with increasing final size representing overall growth rate of the organism during its life cycle.

[40] The contrast in the relationship between size and Mg concentrations in *G. sacculifer* and *G. ruber* suggests, as with boron isotopes, that the presence/absence of the gametogenic calcite plays a role. As we have alluded to above and has been discussed previously in the literature [*Bé*, 1980; *Bé et al.*, 1977] the gametogenic calcite in foraminifers shows different chemical and isotopic compositions partly because it is deposited in an environment with properties different from those where the rest of the skeleton was built (Figure 6), and partly because the mechanism of calcification may be different [*Erez*, 2003]. Electron probe

microanalysis studies have observed low magnesium concentrations in the gametogenic layer of *Globigerina bulloides* [*Elderfield and Ganssen*, 2000], *Globorotalia truncatulinoides* [*Duckworth*, 1977] and *Globorotalia tumida* [*Brown and Elderfield*, 1996]. Using high-resolution LA-ICPMS depth profiling, *Eggins et al.* [2003] found that the gametogenic calcite in *G. sacculifer* is depleted in Mg compared to the ontogenetic calcite, whereas *G. ruber* exhibits little variation in Mg concentrations. However, some studies have also noted exceptionally high Mg/Ca in a thin (1–3 μm) outer rim in *G. sacculifer* [*Nürnberg et al.*, 1996; *Eggins et al.*, 2003; *Sadekov et al.*, 2005] from sediment samples. It is unlikely that this layer represents the gametogenic calcite since it is too thin, but instead it may be an altered layer on the outside of the fossil specimen which also contains clay particles (as evidenced by high Mn and Si) which will be removed during sample cleaning [*Brown and Elderfield*, 1996; *Barker et al.*, 2005] and hence should not influence our results.

[41] Given the low Mg concentrations in the gametogenic calcite, small individuals are expected to have lower bulk Mg/Ca ratios than larger ones because of their higher surface to volume ratios. This higher surface to volume ratio results in a higher relative proportion of gametogenic calcite in small specimen in contrast to large specimen assuming constant thickness of the gametogenic and ontogenetic calcite (D. N. Schmidt, unpublished data, 2007). Only *G. sacculifer* deposits a thick gametogenic calcite; therefore *G. sacculifer* should show a change in Mg/Ca ratio with test size while *G. ruber* should not (Figure 5). Preferential dissolution of the higher Mg/Ca ontogenetic calcite, as discussed previously for the Pacific samples, further explains the larger relative change in Mg/Ca with test size in our Site 806 samples.

6. Conclusions

[42] This study presents a combined analysis of trace elements and δ^{11}B on the same foraminiferal samples allowing an assessment of the environmental and biological controls on these proxies. We have three main conclusions.

[43] 1. For *G. sacculifer* specimens at sites with a thick mixed layer, as in the Pacific Site 806B and the Indian Site RC 14-37PC, δ^{11}B is lower in the gametogenic calcite as a result of water column and microenvironmental pH changes during gametogenesis below the base of the mixed layer. Smaller tests of *G. sacculifer* have a larger relative proportion of gametogenic calcite, which can be accentuated by preferential dissolution of the ontogenetic calcite. This results in a significant variability of δ^{11}B with test size in our Indian and Pacific Sites. Foraminifers in the Atlantic Site 664C, a Site with a thin mixed layer, do not exhibit significant differences in δ^{11}B between gametogenic and ontogenetic calcite. Consequently, δ^{11}B in *G. sacculifer* exhibits little or no size dependence. *G. ruber* has no significant gametogenic calcite and undergoes little or no depth migration during its life cycle; therefore differential dissolution does not alter δ^{11}B in this species in either the Atlantic or Pacific sites. It appears to be a robust species for δ^{11}B paleoproxy work.

[44] 2. Significant variations of B/Ca, U/Ca and Li/Ca are evident with final test size of the foraminifer. We suggest that this may be explained by higher overall growth rate in larger individuals than in small ones, resulting in less efficient discrimination of the trace elements during their incorporation into the calcite lattice in overall faster growing organisms. Site specific variability of B/Ca and U/Ca also reflect differences in ambient carbonate equilibria, but the contrast between the strong site and test size dependence of B/Ca and U/Ca ratios and the largely invariant δ^{11}B in *G. ruber* suggests additional parameters more strongly control the trace element ratios than the isotopic proxy.

[45] 3. Mg/Ca ratios only show test size dependence in *G. sacculifer* suggesting that the overall growth rate of the organisms does not affect the discrimination against Mg. Gametogenic calcite has lower Mg/Ca ratios. Therefore the size related variation of Mg/Ca in *G. sacculifer* but not *G. ruber* is likely due to the presence/absence of gametogenic calcite. Small individuals have a larger proportion of gametogenic calcite because of the relatively large surface area to volume ratios, and consequently, they display lower bulk Mg/Ca ratios.

[46] **Acknowledgments.** We thank B. Hönisch for generously supplying samples for interlaboratory comparison and helpful encouragement during our development of boron isotope measurements. This work was funded by NERC grant NER/A/S/2001/01213, Joint Infrastructure grant number GR3/JIF/46 to the Department of Earth Sciences, and NERC postdoctoral fellowships to Gavin Foster and Daniela Schmidt. Yunyan Ni was supported by an ORS fellowship supplemented by the Department of Earth Sciences, University of Bristol.

References

Al-Ammar, A. S., R. K. Gupta, and R. M. Barnes (2000), Elimination of boron memory effect in inductively coupled plasma-mass spectrometry by ammonia gas injection into the spray chamber during analysis, *Spectrochim. Acta, Part B*, *55*, 629–635.

Anand, P., H. Elderfield, and M. H. Conte (2003), Calibration of Mg/Ca thermometry in planktonic foraminifera from a sediment trap time series, *Paleoceanography*, *18*(2), 1050, doi:10.1029/2002PA000846.

Anderson, O. R., and W. W. Faber (1984), An estimation of calcium carbonate deposition rate in a planktonic foraminifera *Globigerinoides sacculifer* using Ca-45 as a tracer—A recommended procedure for improved accuracy, *J. Foraminiferal Res.*, *14*, 303–308.

Axelsson, M. D., I. Rodushkin, J. Ingri, and B. Öhlander (2002), Multielement analysis of Mn-Fe nodules by ICP-MS: Optimisation of analytical method, *Analyst*, *127*, 76–82.

Barker, S., and H. Elderfield (2002), Foraminiferal calcification response to glacial-interglacial changes in atmospheric CO_2, *Science*, *297*, 833–836.

Barker, S., M. Greaves, and H. Elderfield (2003), A study of cleaning procedures used for foraminiferal Mg/Ca paleothermometry, *Geochem. Geophys. Geosyst.*, *4*(9), 8407, doi:10.1029/2003GC000559.

Barker, S., I. Cacho, H. Benway, and K. Tachikawa (2005), Planktonic foraminiferal Mg/Ca as a

proxy for past oceanic temperatures: A methodological overview and data compilation for the Last Glacial Maximum, *Quat. Sci. Rev.*, *24*, 821–834.

Bassinot, F. C., F. Mélières, M. Gehlen, C. Levi, and L. Labeyrie (2004), Crystallinity of foraminifera shells: A proxy to reconstruct past bottom water CO_3^{2-} changes?, *Geochem. Geophys. Geosyst.*, *5*, Q08D10, doi:10.1029/2003GC000668.

Bé, A. W. H. (1980), Gametogenic calcification in a spinose planktonic foraminifera, *Globigerinoides sacculifer* (Brady), *Mar. Micropaleontol.*, *5*, 283–310.

Bé, A. W. H., et al. (1977), Laboratory and field observation of living planktonic foraminifera, *Micropaleontology*, *23*, 155–179.

Bé, A. W. H., J. K. B. Bishop, M. S. Sverdlove, and W. D. Gardner (1985), Standing stock, vertical distribution and flux of planktonic foraminifera in the Panama Basin, *Mar. Micropaleontol.*, *9*, 307–333.

Benway, H. M., B. A. Haley, G. P. Klinkhammer, and A. C. Mix (2003), Adaptation of a flow-through leaching procedure for Mg/Ca paleothermometry, *Geochem. Geophys. Geosyst.*, *4*(2), 8403, doi:10.1029/2002GC000312.

Berger, W. H., and D. J. W. Piper (1972), Planktonic foraminifera—Differential settling, dissolution, and redeposition, *Limnol. Oceanogr.*, *17*, 275–287.

Berger, W. H., M. C. Bonneau, and F. L. Parker (1982), Foraminifera on the deep-sea-floor—Lysocline and dissolution rate, *Oceanol. Acta*, *5*, 249–258.

Berger, W. H., et al. (1993), Quaternary oxygen isotope record of pelagic foraminifers: Site 806, Ontong Java Plateau, *Proc. Ocean Drill. Program Sci. Results*, *130*, 381–395.

Bijma, J., H. J. Spero, and D. W. Lea (1999), Reassessing foraminiferal stable isotope geochemistry: Impact of the oceanic carbonate system (experimental results), in *Use of Proxies in Paleoceanography: Examples From the South Atlantic*, edited by G. Fischer and G. Wefer, pp. 489–512, Springer, New York.

Bijma, J., B. Hönisch, and R. E. Zeebe (2002), Impact of the oceanic carbonate chemistry on living foraminiferal shell weight: Comment on "Carbonate ion concentration in glacial-age deep waters of the Caribbean Sea" by W. S Broecker and E. Clark, *Geochem. Geophys. Geosyst.*, *3*(11), 1064, doi:10.1029/2002GC000388.

Bonneau, M. C., F. Mélières, and C. Vergnaud-Grazzini (1980), Variations isotopiques (oxygène et carbone) et crystallographiques chez des espèces actuelles de foraminifères planctoniques en fonction de la profondeur de dépôt, *Bull. Soc. Geol. Fr.*, *22*, 791–793.

Boyle, E. A., and L. D. Keigwin (1998), Comparison of Atlantic and Pacific paleochemical records for the last 215,000 years: Changes in deep ocean circulation and chemical inventories, *Earth Planet. Sci. Lett.*, *76*, 135–150.

Brown, S. J., and H. Elderfield (1996), Variations in Mg/Ca and Sr/Ca ratios of planktonic foraminifera caused by postdepositional dissolution: Evidence of shallow Mg-dependent dissolution, *Paleoceanography*, *11*, 543–551.

Caron, D. A., O. R. Anderson, J. L. Lindsey, W. W. Faber Jr., and E. L. Lim (1990), Effects of gametogenesis on test structure and dissolution of some spinose planktonic foraminifera and implications for test preservation, *Mar. Micropaleontol.*, *16*, 93–116.

Cutani, Y. (1984), Sr/Ca ratios in marine carbonates from the Gulf of Eilat (in Hebrew), M. S. thesis, Hebrew Univ. of Jerusalem, Jerusalem.

Dekens, P. S., D. W. Lea, D. K. Pak, and H. J. Spero (2002), Core top calibration of Mg/Ca in tropical foraminifera: Refining paleotemperature estimation, *Geochem. Geophys. Geosyst.*, *3*(4), 1022, doi:10.1029/2001GC000200.

Delaney, M. L., A. W. H. Bé, and E. A. Boyle (1985), Li, Sr, Mg, and Na in foraminiferal calcite shells from laboratory culture, sediment traps, and sediment cores, *Geochim. Cosmochim. Acta*, *49*, 1327–1341.

Deyhle, A., and A. Kopf (2004), Possible influence of clay contamination on B isotope geochemistry of carbonaceous samples, *Appl. Geochem.*, *19*, 737–745.

Duckworth, D. L. (1977), Magnesium concentration in the tests of the planktonic foraminifer *Globorotalia truncatulinoides*, *J. Foraminiferal Res.*, *7*, 304–312.

Eggins, S., P. De Deckker, and J. Marshall (2003), Mg/Ca variation in planktonic foraminifera tests: Implications for reconstructing palaeo-seawater temperature and habitat migration, *Earth Planet. Sci. Lett.*, *212*, 291–306.

Elderfield, H., and G. Ganssen (2000), Past temperature and $\delta^{18}O$ of surface ocean waters inferred from foraminiferal Mg/Ca ratios, *Nature*, *405*, 442–445.

Elderfield, H., M. Vautravers, and M. Cooper (2002), The relationship between shell size and Mg/Ca, Sr/Ca, $\delta^{18}O$, and $\delta^{13}C$ of species of planktonic foraminifera, *Geochem. Geophys. Geosyst.*, *3*(8), 1052, doi:10.1029/2001GC000194.

Erez, J. (2003), The source of ions for biomineralization in foraminifera and their implications for paleoceanographic proxies, *Rev. Mineral. Geochem.*, *54*, 115–149.

Foster, G., Y. Ni, B. Haley, and T. Elliott (2006), Accurate and precise isotopic measurement of sub-nanogram sized samples of foraminiferal hosted boron by total evaporation NTIMS, *Chem. Geol.*, *230*, 161–174.

Hall, J. M., and L. H. Chan (2004), Li/Ca in multiple species of benthic and planktonic foraminifera: Thermocline, latitudinal, and glacial-interglacial variation, *Geochim. Cosmochim. Acta*, *68*, 529–545.

Hemleben, C., M. Spindler, and O. R. Anderson (1989), *Modern Planktonic Foraminifera*, Springer, New York.

Hemming, N. G., and G. N. Hanson (1992), Boron isotopic composition and concentration in modern marine carbonates, *Geochim. Cosmochim. Acta*, *56*, 537–543.

Henderson, G. M. (2002), New oceanic proxies for paleoclimate, *Earth Planet. Sci. Lett.*, *203*, 1–13.

Hönisch, B., and N. G. Hemming (2004), Ground-truthing the boron isotope paleo-pH proxy in planktonic foraminifera shells: Partial dissolution and shell size effects, *Paleoceanography*, *19*, PA4010, doi:10.1029/2004PA001026.

Hönisch, B., and N. G. Hemming (2005), Surface ocean pH response to variations in *p*CO2 through two full glacial cycles, *Earth Planet. Sci. Lett.*, *236*, 305–314.

Hönisch, B., J. Bijma, A. D. Russell, H. J. Spero, M. R. Palmer, R. E. Zeebe, and A. Eisenhauer (2003), The influence of symbiont photosynthesis on the boron isotopic composition of foraminifera shells, *Mar. Micropaleontol.*, *928*, 1–10.

Kakihana, H., et al. (1977), Fundamental studies on the ion-exchange separation of boron isotopes, *Bull. Chem. Soc. Jpn.*, *50*, 158–163.

Kemle-von Mücke, S., and H. Oberhänsli (1999), The distribution of living planktonic foraminifera in relation to southeast Atlantic oceanography, in *Use of Proxies in Paleoceanography: Examples From the South Atlantic*, edited by G. Fischer and G. Wefer, pp. 91–115, Springer, New York.

Kimoto, K., H. Takaoka, M. Oda, M. Ikehara, H. Matsuoka, M. Okada, T. Oba, and A. Taira (2003), Carbonate dissolution and planktonic foraminiferal assemblages observed in three piston cores collected above the lysocline in the western equatorial Pacific, *Mar. Micropaleontol.*, *47*, 227–251.

Klochko, K., A. J. Kaufman, W. Yao, R. H. Byrne, and J. A. Tossell (2006), Experimental measurement of boron isotope fractionation in seawater, *Earth Planet. Sci. Lett.*, *248*, 261–270.

Lea, D. W., T. A. Mashiotta, and H. J. Spero (1999), Controls on magnesium and strontium uptake in planktonic foraminifera determined by live culturing, *Geochim. Cosmochim. Acta*, *63*, 2369–2379.

Liu, Y., and J. A. Tossell (2005), Ab initio molecular orbital calculations for boron isotope fractionations on boric acids and borates, *Geochim. Cosmochim. Acta*, *69*, 3995–4006.

Marriott, C. S., G. M. Henderson, N. S. Belshawa, and A. W. Tudhope (2004a), Temperature dependence of δ^7Li, $\delta^{44}Ca$ and Li/Ca during growth of calcium carbonate, *Earth Planet. Sci. Lett.*, *222*, 615–624.

Marriott, C. S., G. M. Henderson, R. Crompton, M. Staubwasser, and S. Shaw (2004b), Effect of mineralogy, salinity, and temperature on Li/Ca and Li isotope composition of calcium carbonate, *Chem. Geol.*, *212*, 5–15.

Ni, Y. (2006), Evaluation of boron isotopes and trace element abundances in planktonic foraminifers as palaeo-oceanographic proxies, Ph.D. thesis, 240 pp., Univ. of Bristol, U. K.

Nürnberg, D., J. Bijma, and C. Hemleben (1996), Assessing the reliability of magnesium in foraminiferal calcite as a proxy for water mass temperatures, *Geochim. Cosmochim. Acta*, *60*, 803–814.

Pagani, M., D. Lemarchand, A. Spivack, and J. Gaillardet (2005), A critical evaluation of the boron isotope-pH proxy: The accuracy of ancient ocean pH estimates, *Geochim. Cosmochim. Acta*, *69*, 953–961.

Palmer, M. R., and P. N. Pearson (2003), A 23,000-year record of surface water pH and pCO_2 in the western equatorial Pacific Ocean, *Science*, *300*, 480–482.

Palmer, M. R., P. N. Pearson, and S. J. Cobb (1998), Reconstructing past ocean pH-depth profiles, *Science*, *282*, 1468–1471.

Peterson, L. C., and W. L. Prell (1985), Carbonate dissolution in recent sediments of the eastern equatorial Indian Ocean—Preservation patterns and carbonate loss above the lysocline, *Mar. Geol.*, *64*, 259–290.

Raymo, M. E., D. W. Oppo, and W. Curry (1997), The mid-Pleistocene climate transition: A deep sea carbon isotopic perspective, *Paleoceanography*, *12*, 546–559.

Rickaby, R. E. M., S. P. Schrag, I. Zondervan, and U. Riebesell (2002), Growth rate dependence of Sr incorporation during calcification of *Emiliania huxleyi*, *Global Biogeochem. Cycles*, *16*(1), 1006, doi:10.1029/2001GB001408.

Rink, S., M. Kuhl, J. Bijma, and H. J. Spero (1998), Microsensor studies of photosynthesis and respiration in the symbiotic foraminifer *Orbulina universa*, *Mar. Biol.*, *131*, 583–595.

Rosenthal, Y., M. P. Field, and R. M. Sherrell (1999), Precise determination of elemental/calcium ratios in calcareous samples using sector field inductively coupled plasma mass spectrometry, *Anal. Chem.*, *71*, 3248–3253.

Russell, A. D., S. Emerson, A. C. Mix, and L. C. Peterson (1996), The use of foraminiferal uranium/calcium ratios as an indicator of changes in seawater uranium content, *Paleoceanography*, *11*, 649–663.

Russell, A. D., B. Hönisch, H. J. Spero, and D. W. Lea (2004), Effects of seawater carbonate ion concentration and temperature on shell U, Mg, and Sr in cultured planktonic foraminifera, *Geochim. Cosmochim. Acta*, *68*, 4347–4361.

Sadekov, A. Y., S. M. Eggins, and P. De Deckker (2005), Characterization of Mg/Ca distributions in planktonic foraminifera species by electron microprobe mapping, *Geochem. Geophys. Geosyst.*, *6*, Q12P06, doi:10.1029/2005GC000973.

Sanyal, A., N. G. Hemming, G. N. Hanson, and W. S. Broecker (1995), Evidence for a higher pH in the glacial ocean from boron isotopes in foraminifera, *Nature*, *373*, 234–236.

Sanyal, A., N. G. Hemming, W. S. Broecker, D. W. Lea, H. J. Spero, and G. N. Hanson (1996), Oceanic pH control on the boron isotopic composition of foraminifera: Evidence from culture experiments, *Paleoceanography*, *11*, 513–517.

Sanyal, A., M. Nugent, R. J. Reeder, and J. Bijma (2000), Seawater pH control on the boron isotopic composition of calcite: Evidence from inorganic calcite precipitation experiments, *Geochim. Cosmochim. Acta*, *64*, 1551–1555.

Sanyal, A., J. Bijma, H. Spero, and D. W. Lea (2001), Empirical relationship between pH and boron isotopic composition of Globigerinoides sacculifer: Implications for the boron isotope paleo-pH proxy, *Paleoceanography*, *16*, 515–519.

Schmidt, D. N., and S. Kasemann (2006), Biology of boron isotopes in planktic foraminifers: New understanding based on in situ analysis (SIMS), *Geochim. Cosmochim. Acta*, *70*, 10.

Schmidt, G. A., and S. Mulitza (2002), Global calibration of ecological models for planktic foraminifera from coretop carbonate oxygen-18, *Mar. Micropaleontol.*, *44*, 125–140.

Schmidt, D. N., S. Renaud, J. Bollmann, R. Schiebel, and R. Thierstein (2004), Size distribution of Holocene planktic foraminifer assemblages: Biogeography, ecology and adaptation, *Mar. Micropaleontol.*, *50*, 319–338.

Segev, E., and J. Erez (2006), Effect of Mg/Ca ratio in seawater on shell composition in shallow benthic foraminifera, *Geochem. Geophys. Geosyst.*, *7*, Q02P09, doi:10.1029/2005GC000969.

Spero, H. J., and S. L. Parker (1985), Photosynthesis in the symbiotic planktonic foraminifer *Orbulina universa*, and its potential contribution to oceanic primary productivity, *J. Foraminiferal Res.*, *15*, 273–281.

Spero, H. J., I. Lerche, and D. F. Williams (1991), Opening the carbon isotope "vital effect" box, 2. Quantitative model for interpreting foraminiferal carbon isotope data, *Paleoceanography*, *6*, 639–655.

Spivack, A. J., C.-F. You, and H. J. Smith (1993), Foraminiferal boron isotope ratios as a proxy for surface ocean pH over the past 21 Myr, *Nature*, *363*, 149–151.

Takahashi, T., et al. (2002), Global sea-air CO_2 flux based on climatological surface ocean pCO_2, and seasonal biological and temperature effects, *Deep Sea Res., Part II*, *49*, 1601–1622.

Tossell, J. A. (2005), Boric acid, "carbonic" acid, and N-containing oxyacids in aqueous solution: Ab initio studies of structure, *p*Ka, NMR shifts, and isotopic fractionations, *Geochim. Cosmochim. Acta*, *69*, 5647–5658.

Vengosh, V., A. R. Chivas, and M. T. McCulloch (1989), Direct determination of boron and chlorine isotopic compositions in geological materials by negative thermal-ionisation mass spectrometry, *Chem. Geol.*, *79*, 333–343.

Wolf-Gladrow, D. A., J. Bijma, and R. E. Zeebe (1999), Model simulation of the carbonate chemistry in the microenvironment of symbiont bearing foraminifera, *Mar. Chem.*, *64*, 181–198.

Yu, J., H. Elderfield, and B. Hönisch (2007), B/Ca in planktonic foraminifera as a proxy for surface seawater pH, *Paleoceanography*, *22*, PA2202, doi:10.1029/2006PA001347.

Zeebe, R. E. (2005), Stable boron isotope fractionation between dissolved $B(OH)_3$ and $B(OH)_4^-$, *Geochim. Cosmochim. Acta*, *69*, 2753–2766.

Zeebe, R. E., and D. Wolf-Gladrow (2001), *CO_2 in Seawater: Equilibrium, Kinetics, Isotopes*, *Oceanogr. Ser.*, vol. 65, Elsevier, New York.

Zeebe, R. E., A. Sanyal, J. D. Ortiz, and D. A. Wolf-Gladrow (2001), A theoretical study of the kinetics of the boric acid-borate equilibrium in seawater, *Mar. Chem.*, *73*, 113–124.

Zeebe, R. E., D. A. Wolf-Gladrow, J. Bijma, and B. Hönisch (2003), Vital effects in foraminifera do not compromise the use of $\delta^{11}B$ as a paleo-pH indicator: Evidence from modeling, *Paleoceanography*, *18*(2), 1043, doi:10.1029/2003PA000881.

T. Bailey, National Museums and Galleries of Wales, Cathays Park, CF10 3NP Cardiff, UK.

C. Coath, T. Elliott, and G. L. Foster, Bristol Isotope Group, Department of Earth Sciences, University of Bristol, Wills Memorial Building, Queens Road, BS8 1RJ Bristol, UK. (g.l.foster@bristol.ac.uk)

B. Haley, IFM-GEOMAR, Wischhofstrasse 1-3, D-24148 Kiel, Germany.

Y. Ni, Research Institute of Petroleum Exploration and Development, Beijing 100083, China.

P. Pearson, School of Earth, Ocean and Planetary Sciences, Cardiff University, Main Building, Park Place, CF10 3YE Cardiff, UK.

D. N. Schmidt, Department of Earth Sciences, University of Bristol, Wills Memorial Building, Queens Road, BS8 1RJ Bristol, UK.